Cosmological observables in galaxy redshift survey datasets

Florian Beutler

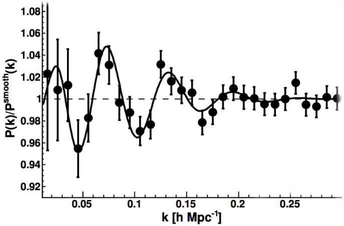

European Research Council
Established by the European Commission

THE ROYAL SOCIETY

THE UNIVERSITY OF EDINBURGH

Royal Society University Research Fellow

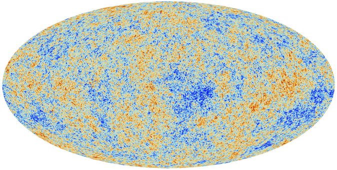

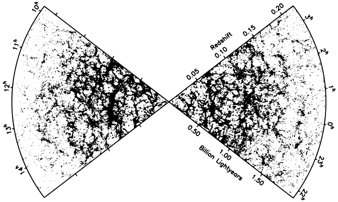

1. Measure the position of galaxies (RA, DEC + redshift).
2. The CMB tells us the initial conditions for today's distribution of matter.
3. How the initial density fluctuations in the CMB evolved from redshift $z = 1100$ to today depends on Ω_m, Ω_Λ, H_0 etc.

From a point distribution to a power spectrum

- Overdensity-field:

$$\delta(\mathbf{x}) = \frac{\rho(\mathbf{x}) - \overline{\rho}}{\overline{\rho}}$$

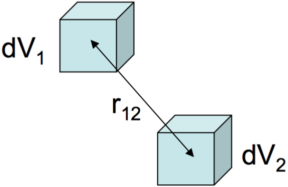

- Two-point function:

$$\xi(\mathbf{r}) \overset{\text{homogeneity}}{=} \langle \delta(\mathbf{x}+\mathbf{r})\delta(\mathbf{x}) \rangle \begin{cases} \overset{\text{isotropy}}{=} & \xi(r) \\ \overset{\text{anisotropy}}{=} & \xi_\ell(r) = \int_{-1}^{1} d\mu\, \xi(r,\mu)\mathcal{L}_\ell(\mu) \end{cases}$$

- ...and in Fourier-space:

$$\boxed{P_\ell(k) = 4\pi(-i)^\ell \int r^2 dr\, \xi_\ell(r) j_\ell(kr)}$$

From a point distribution to a bispectrum

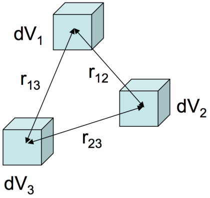

- Overdensity-field:

$$\delta(\mathbf{x}) = \frac{\rho(\mathbf{x}) - \overline{\rho}}{\overline{\rho}}$$

- Three-point function:

$$\xi(\mathbf{r}_1, \mathbf{r}_2) \overset{\text{homogeneity}}{=} \langle \delta(\mathbf{x} + \mathbf{r}_1)\delta(\mathbf{x} + \mathbf{r}_2)\delta(\mathbf{x}) \rangle \begin{cases} \overset{\text{isotropy}}{=} & \xi_L(r_1, r_2) \\ \overset{\text{anisotropy}}{\longrightarrow} & \xi_{\ell_1 \ell_2 L}(r_1, r_2) \end{cases}$$

- ...and in Fourier-space:

$$\boxed{B_{\ell_1 \ell_2 L}(k_1, k_2) = (4\pi)^2(-i)^{\ell_1+\ell_2} \int r_1^2 dr_1 \int r_2^2 dr_2 \xi_{\ell_1 \ell_2 L}(r_1, r_2) j_{\ell_1}(k_1 r_1) j_{\ell_2}(k_2 r_2)}$$

$\rightarrow$ Public Python/C++ package **Triumvirate**, arXiv:2304.03643
`https://triumvirate.readthedocs.io/en/latest/`

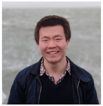

Extracting cosmological information

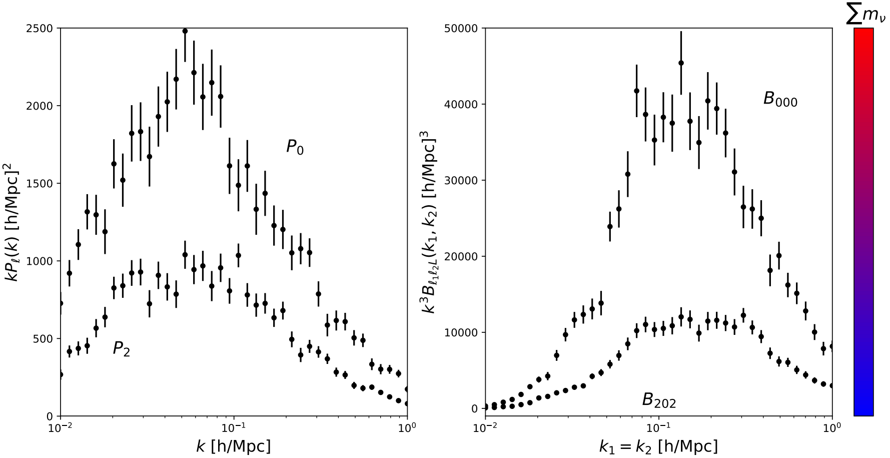

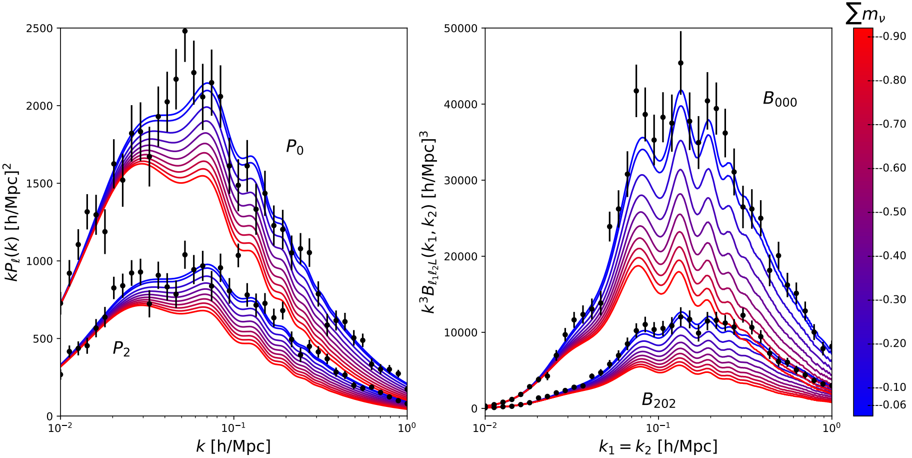

2500
2000
1500
1000
500
0
$kP_\ell(k)$ [h/Mpc]^2
P_0
P_2
10^{-2}
10^{-1}
10^0
k [h/Mpc]
50000
40000
30000
20000
10000
0
$k^3 B_{\ell_1\ell_2 L}(k_1, k_2)$ [h/Mpc]^3
B_{000}
B_{202}
$k_1 = k_2$ [h/Mpc]
$\sum m_\nu$
0.90
0.80
0.70
0.60
0.50
0.40
0.30
0.20
0.10
0.06

The BOSS galaxy survey

- Third version of the Sloan Digital Sky Survey (SDSS-III)
- Spectroscopic survey optimized for the measurement of Baryon Acoustic Oscillations (BAO)
- The galaxy sample includes 1 100 000 galaxy redshifts in the range $0.2 < z < 0.75$
- The effective volume is $\sim 6\,\mathrm{Gpc}^3$
- 1000 fibres/redshifts per pointing

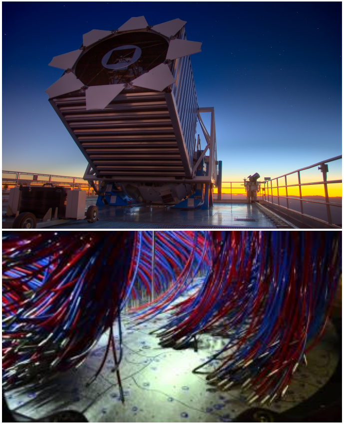

- Mayall 4m telescope at Kitt Peak, Arizona
- 5000 fibres/pointing
- Will observe 3 types of galaxies (LRGs/ELGs/QSOs) + BGS
- 30 - 40 million galaxies in total
- z < 1.8 with galaxies and z < 3.5 with Ly-α forest

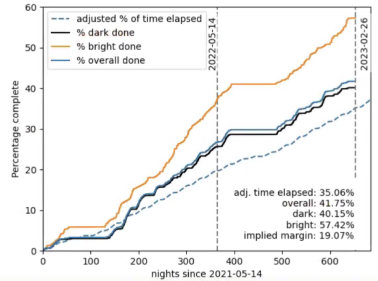

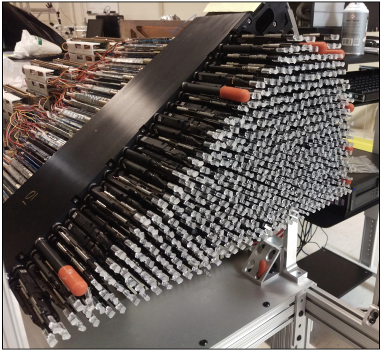

Summer 2022 at Kitt Peak

The ESA Euclid mission

- Launched in July 2023 → L2 point
- Space-based weak lensing + gal. clustering survey over 15 000 deg^2
- 30 million emission line galaxies over the redshift range 0.7 to 2.0
- Slitless spectroscopy (grism)

ESA's Euclid mission
@ESA_Euclid

🚀 Liftoff for the #DarkUniverse 🕵️ detective that aims to shed light on the nature of #DarkMatter & #DarkEnergy

👏 #ESAEuclid

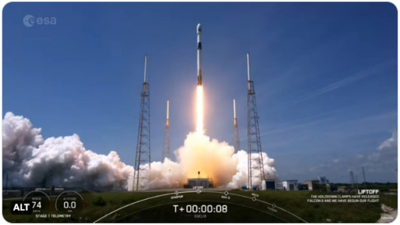

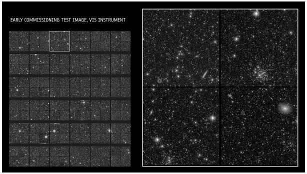

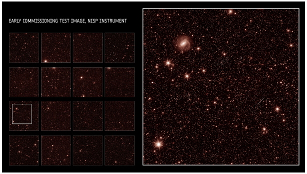

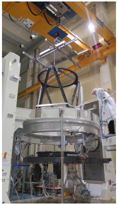

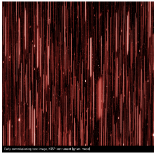

Euclid first images

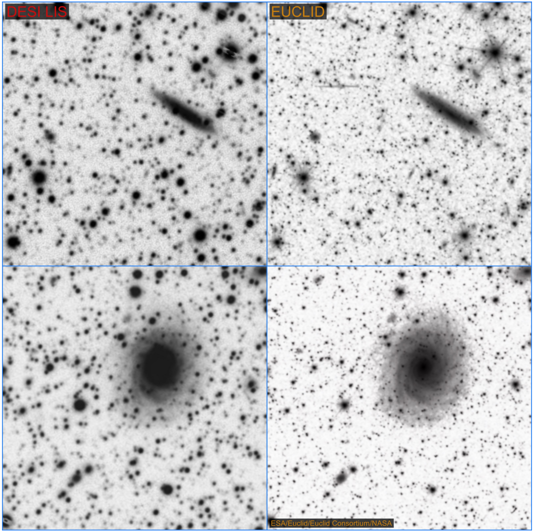

What are Baryon Acoustic Oscillations?

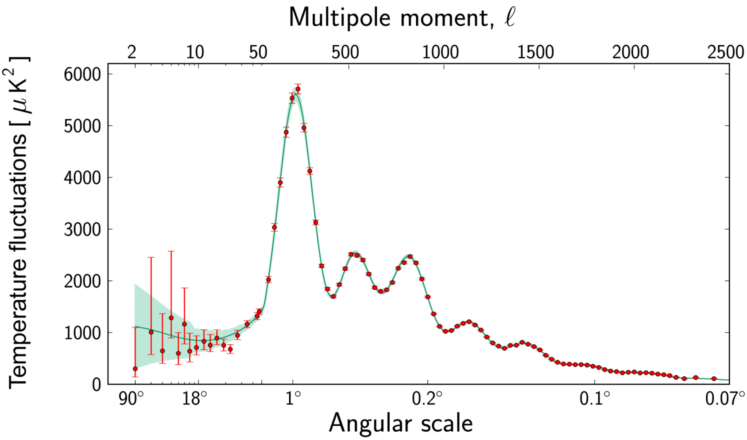

Planck collaboration

Baryon Acoustic Oscillations in BOSS

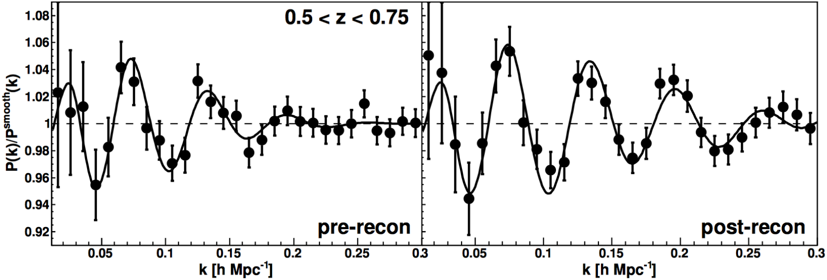

- BAO are the most robust observable we can extract from LSS
- The observables are

$$(1+z)D_A(z)/r_d = \int_0^z \frac{cdz'}{r_d H(z')}$$

$$H(z)r_d = H_0 r_d \sqrt{\Omega_m(1+z)^3 + \Omega_\Lambda + \Omega_k(1+z)^2}$$

- We require a calibration of the ruler to constrain H_0 (+ cos. model to extrapolate to $z = 0$)

BAO and H_0

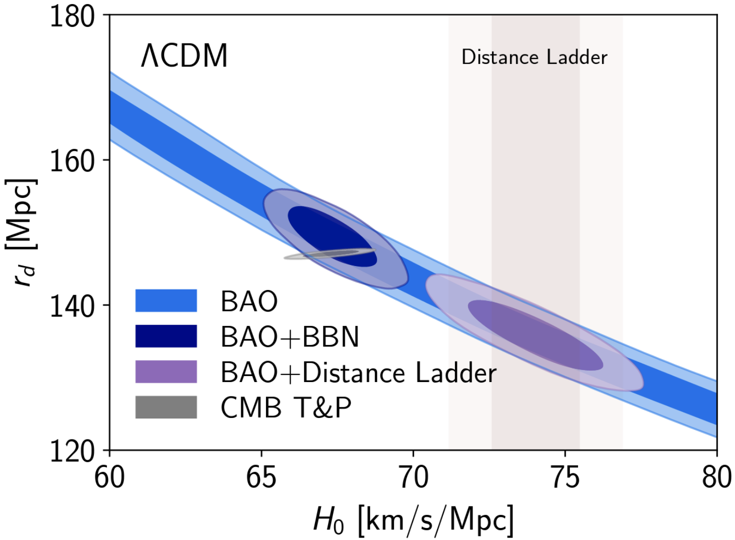

Alam et al. 2020

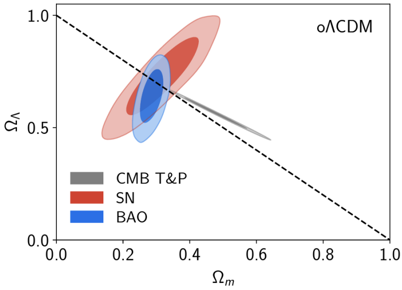

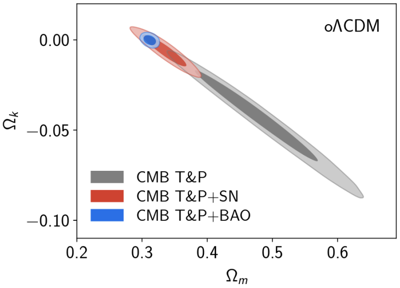

- Planck: $\Omega_k = -0.044^{+0.019}_{-0.014}$
- Planck+BAO: $\Omega_k = -0.0001 \pm 0.0018$

Alam et al. (2020)

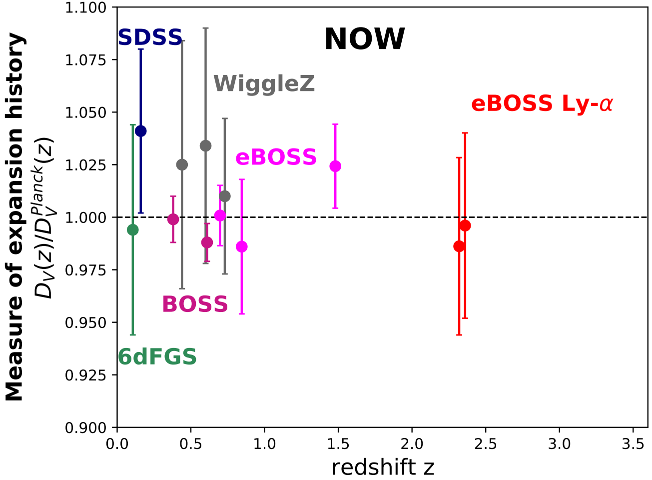

$$D_V(z) = \left[(1+z)^2 D_A^2(z) \frac{cz}{H(z)}\right]^{1/3}$$

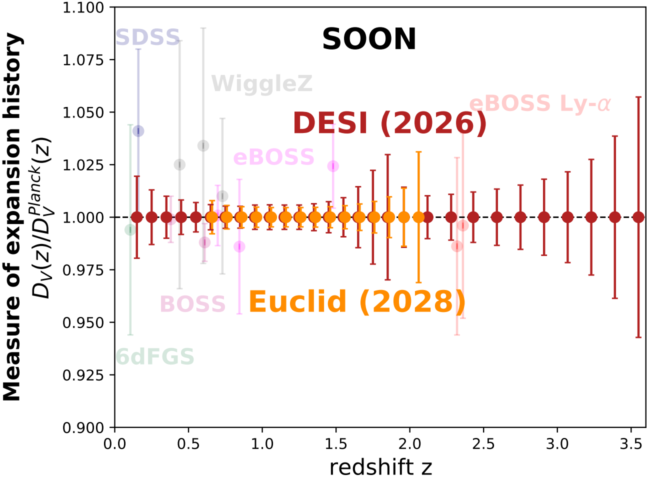

$$D_V(z) = \left[(1+z)^2 D_A^2(z)\frac{cz}{H(z)}\right]^{1/3}$$

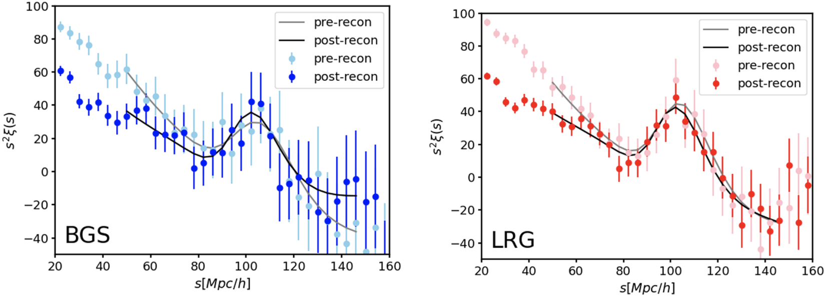

Table 3. BAO key fitting results for DESI-M2 LRGs and BGS.

Sample	Reconstruction	BAO Detection Significance	$\alpha + \Delta\alpha$	$\min(\chi^2)$/dof
DESI-M2 LRG	Pre-recon	5.170	0.987 ± 0.016	15.619 / 20
	Post-recon	5.050	1.000 ± 0.017	13.463 / 20
DESI-M2 BGS	Pre-recon	2.337	0.980 ± 0.040	13.172 / 20
	Post-recon	2.963	1.001 ± 0.026	16.724 / 20

- 2 months of data (unblinded), no cosmological analysis
- 110k galaxies in BGS and 260k in the LRG sample
- Forecasting 0.29% error on the BAO between $0.4 < z < 1.1$

Moon et al. (2023)

What are redshift-space distortions?

Many more observables, RSD, modified gravity, testing inflation, number of relativistic particles in the early Universe

The densities along the line-of-sight are enhanced due to the velocity field

$$\delta_g(k) = b_1\delta_m(k) - \mu^2\nabla\cdot\mathbf{v}$$
$$= \delta_m(k)(b_1 + f\mu^2)$$

→ Introduces a quadrupole
→ Sensitive to cosmology since

$$f = \frac{\partial \ln D}{\partial \ln a} \approx \Omega_m^{0.55}$$

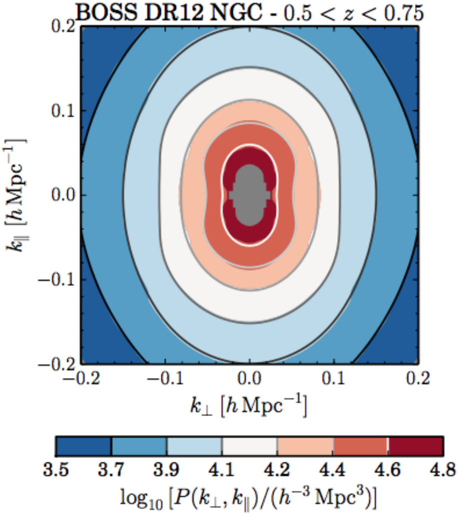

How to extract this information

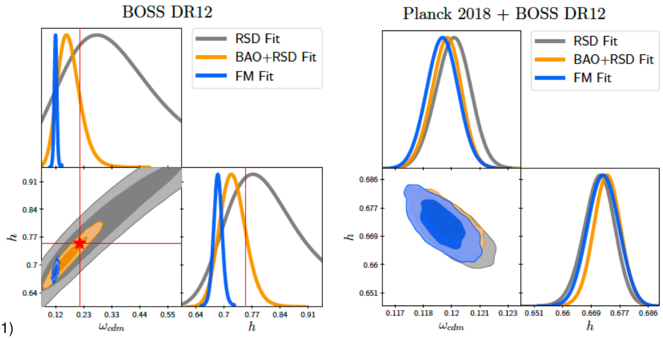

Brieden et al. (2021)

- The original BOSS analysis extracted BAO and RSD information ($f\sigma_8$, $D_A(z)/r_d$, $H(z)r_d$)
- Recently there was a push for full-shape fits, which can extract additional information from the slope of the power spectrum
- Such information can be extracted from template fits by an extension of 1 or 2 parameters (*ShapeFit*, Brieden et al. 2021)
- How to combine post-recon BAO with a full-shape analysis (Chen et al. 2022)

Testing inflation through primordial non-Gaussianity

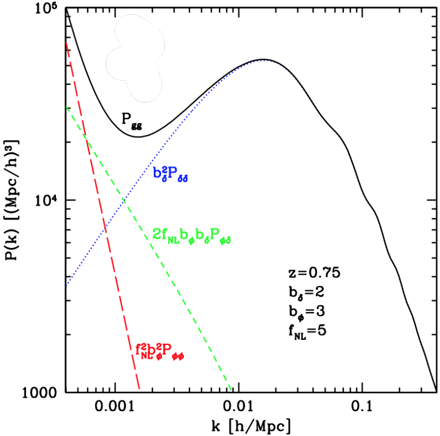

$$\phi_{\rm p} = \phi + f_{\rm NL}^{\rm loc}(\phi^2 - \langle\phi^2\rangle)$$

$$\delta_g(k) = \delta_m(k)\left(b_1 + f\mu^2 + \frac{b_\phi f_{\rm NL}^{\rm loc}\alpha}{k^2}\right) \longrightarrow P_g \propto \frac{b_\phi f_{\rm NL}^{\rm loc}}{k^2}$$

Dalal et al (2008), McDonald (2008)

Primordial non-Gaussianity with LSS

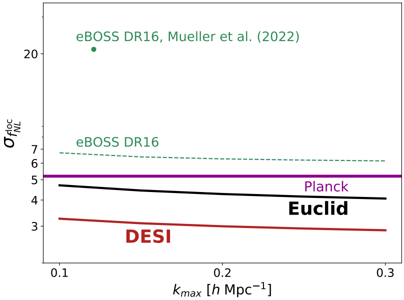

- eBOSS DR16 QSOs: $f_{\rm NL}^{\rm loc} = 12 \pm 21$ (68 C.L.) excluding small k modes and QSOs above $z > 2.2$ (Mueller et al. 2022)
- Theoretical systematics e.g. $b_\phi f_{\rm NL}^{\rm loc}$ degeneracy (Barreira 2022), rel. effects (Castorina & di Dio 2022)
- **SPHEREx** forecasts $\longrightarrow \sigma_{f_{\rm NL}^{\rm loc}} < 0.87$ (with bispectrum 0.23) (Dore et al. 2015)
- BOSS DR12 constraints from the **bispectrum** are $f_{\rm NL}^{\rm loc} = -30 \pm 29$ (68 C.L.) (D'Amico et al. 2022, Cabass et al. 2022)

Non local PNG from BOSS

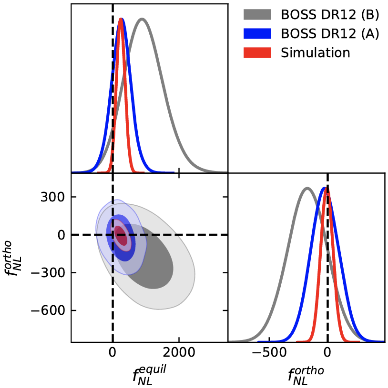

Cabass et al. (2022),

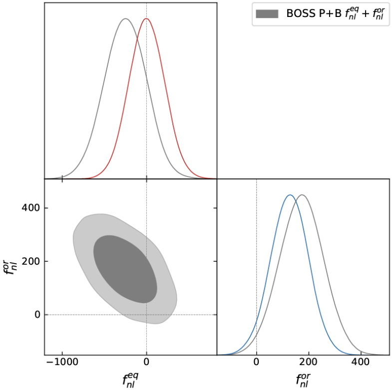

D'Amico et al. (2022)

- Planck 2018: $f_{\rm NL}^{\rm eq} = -26 \pm 47$; $f_{\rm NL}^{\rm ortho} = -38 \pm 24$
- Not yet competitive with the CMB but proof of principle
- **SPHEREx** forecasts $\sigma_{f_{\rm NL}^{\rm eq}} \sim 7$ (Dore et al. 2015)

Testing inflation through primordial features

$$P_{\zeta,0}(k) = \frac{2\pi^2}{k^3}\mathcal{P}_{\zeta,0}(k) = \frac{2\pi^2 A_s}{k^3}\left(\frac{k}{k_*}\right)^{n_s-1}$$

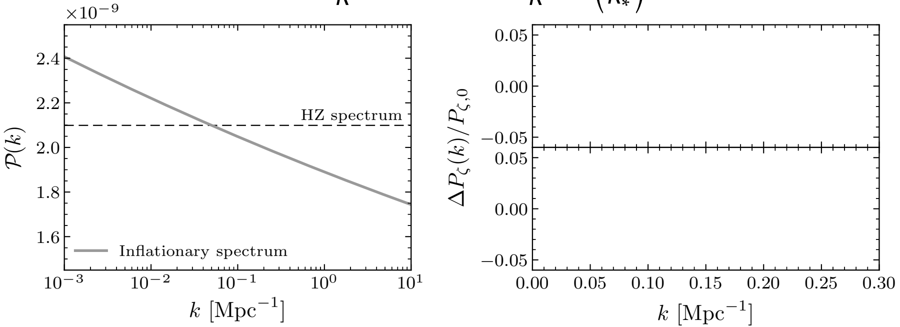

- Feature(s) in the inflationary potential can introduce features in the primordial power spectrum, which might still be detectable today.
- Sharp features can lead to linear oscillations, while periodic features lead to log-oscillations.
- Such features are predicted by many popular inflationary models like monodromy inflation, brane inflation, axion inflation etc.

Testing inflation through primordial features

$$P_{\zeta,0}(k) = \frac{2\pi^2}{k^3}\mathcal{P}_{\zeta,0}(k) = \frac{2\pi^2 A_s}{k^3}\left(\frac{k}{k_*}\right)^{n_s-1}$$

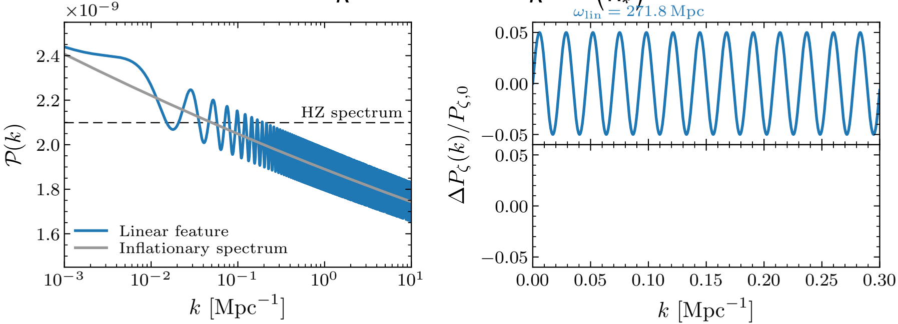

- Feature(s) in the inflationary potential can introduce features in the primordial power spectrum, which might still be detectable today.
- Sharp features can lead to linear oscillations, while periodic features lead to log-oscillations.
- Such features are predicted by many popular inflationary models like monodromy inflation, brane inflation, axion inflation etc.

Testing inflation through primordial features

$$P_{\zeta,0}(k) = \frac{2\pi^2}{k^3}\mathcal{P}_{\zeta,0}(k) = \frac{2\pi^2 A_s}{k^3}\left(\frac{k}{k_*}\right)^{n_s-1}$$

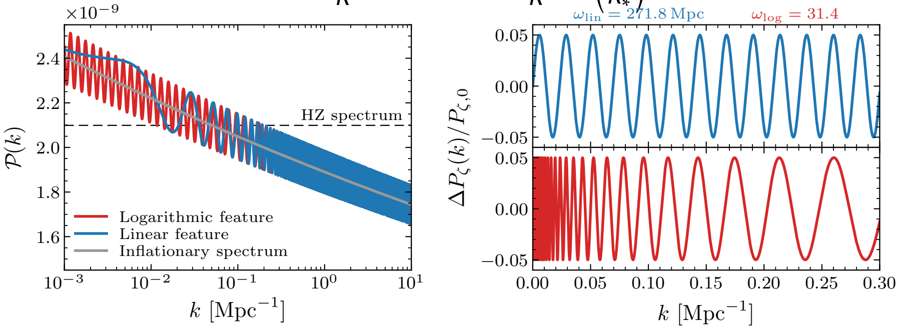

- Feature(s) in the inflationary potential can introduce features in the primordial power spectrum, which might still be detectable today.
- Sharp features can lead to linear oscillations, while periodic features lead to log-oscillations.
- Such features are predicted by many popular inflationary models like monodromy inflation, brane inflation, axion inflation etc.

Testing inflation through primordial features

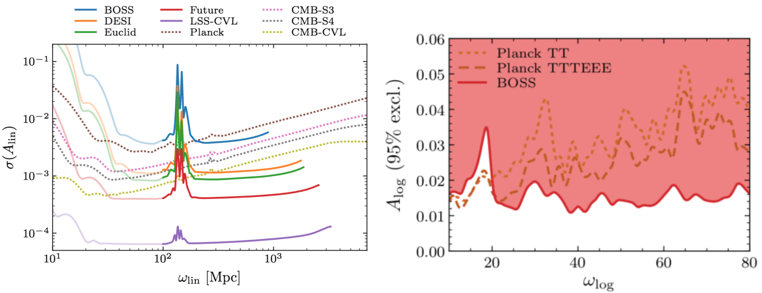

- Here we use a model-independent approach based on

$$\frac{\Delta P_\zeta}{P_\zeta} = \begin{cases} A^{\cos}\cos\left[\omega_{\log}\log\left(\frac{k}{0.05}\right)\right] + A^{\sin}\sin\left[\omega_{\log}\log\left(\frac{k}{0.05}\right)\right], \\ A^{\cos}\cos\left[\omega_{\rm lin}k\right] + A^{\sin}\sin\left[\omega_{\rm lin}k\right] \end{cases}$$

- LSS is more powerful than the CMB on small frequencies, while the CMB can access much higher frequencies
- DESI is going to provide constraints which cannot be accessed even by a CVL CMB experiment

Further linear corrections

$$\delta_g(k) = \delta_m(k)\left(b_1 + f\mu^2\right)$$

- Detecting some of these terms can test theories which modify the Euler equation ($\frac{1}{\mathcal{H}}\partial_r\Psi = \frac{1}{\mathcal{H}}\dot{v}_{||} + v_{||}$) (Bonvin & Fleury 2018)
- Most of these terms are strongly suppressed in the std. 2-pt correlators (e.g. $(\mathcal{H}/k)^2 \sim 10^{-5}$ at $k = 0.1h/\mathrm{Mpc}$ in the power spectrum)

Yoo et al. (2010), Bonvin & Durrer (2011), Challinor & Lewis (2011)

Further linear corrections

$$\delta_g(k) = \delta_m(k)\left(b_1 + f\mu^2\right) - \overbrace{\int_0^r dr' \frac{r-r'}{rr'}\Delta_\Omega(\Phi+\Psi)}^{\text{Lensing}}$$

$$+ \overbrace{\left(1 - \frac{\dot{\mathcal{H}}}{\mathcal{H}^2} - \frac{2}{r\mathcal{H}}\right)v_\parallel + \frac{1}{\mathcal{H}}\dot{v}_\parallel}^{\text{Doppler}} + \overbrace{\frac{1}{\mathcal{H}}\partial_r\Psi}^{\text{grav. redshift}}$$

$$\left.\begin{aligned} &+\Psi - 2\Phi + \frac{1}{\mathcal{H}}\dot{\Phi} + \frac{2}{r}\int_0^r dr'(\Phi+\Psi) \\ &+\left(\frac{\dot{\mathcal{H}}}{\mathcal{H}^2} + \frac{2}{r\mathcal{H}}\right)\left[\Psi + \int_0^r dr'(\dot{\Phi}+\dot{\Psi})\right] \end{aligned}\right\}\text{Potential}$$

- Detecting some of these terms can test theories which modify the Euler equation ($\frac{1}{\mathcal{H}}\partial_r\Psi = \frac{1}{\mathcal{H}}\dot{v}_\parallel + v_\parallel$) (Bonvin & Fleury 2018)
- Most of these terms are strongly suppressed in the std. 2-pt correlators (e.g. $(\mathcal{H}/k)^2 \sim 10^{-5}$ at $k = 0.1h/\text{Mpc}$ in the power spectrum)

Yoo et al. (2010), Bonvin & Durrer (2011), Challinor & Lewis (2011)

DESI-BGS forecasts for relativistic effects

$$P_1(k,z) \overset{(\mathcal{R}^X=\mathcal{R}^Y)}{=} i\Delta b_1 \frac{\mathcal{H}}{k}\left(f\mathcal{R} + \frac{3}{2}\Omega_m\right) D^2 P(k)\,,$$

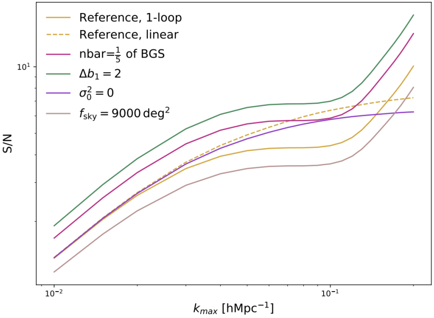

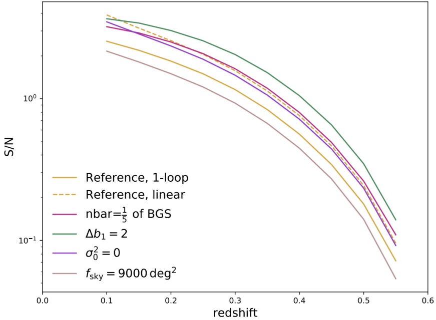

$$\left(\frac{S}{N}\right)^2 = \frac{1}{4\pi^2}\sum_i^{z_{\rm bins}} V(z_i)\int_{k_{\rm min}}^{k_{\rm max}} dk\,k^2 \frac{\left|P_1^{XY}(k,z_i)\right|^2}{\sigma_{P_1}^2(k,z_i)}$$

The Hubble tension and LSS

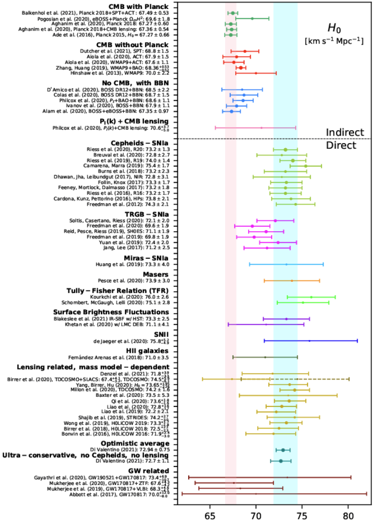

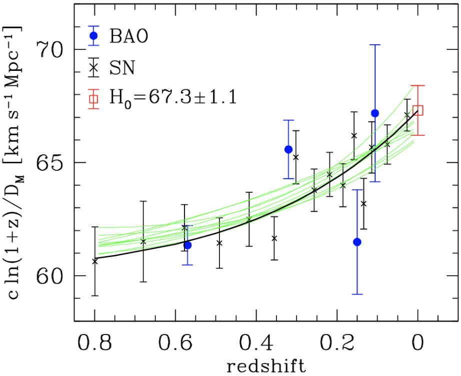

Equality-based constraints: $H_0 = 64.8^{+2.2}_{-2.5}$ km/s Mpc (Philcox et al. 2022)

Valentino et al. (2021), Aubourg et al (2015)

- **Dark Energy Spectroscopic Instrument (DESI; primarily z<1.5)**
  - Baryon Acoustic Oscillations (BAO) and Redshift Space Distortions (RSD)
- **DESI-II (primarily z>2)**
  - As powerful as DESI, but at z>2
  - Early dark energy and growth of structure in matter-dominated regime
  - Synergies with other Cosmic Frontier experiments
- **Spec-S5**
  - Primordial physics (more constraining than the CMB in key areas)

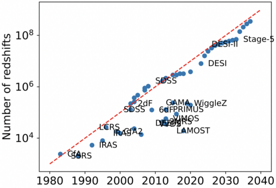

Schlegel at P5

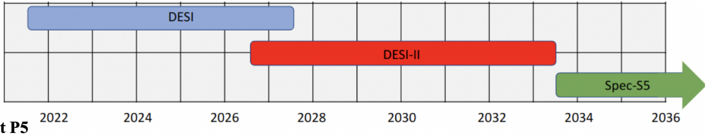

Dawson at P5

13

- Spec-S5 → 6.5m aperture, 20k fibres
- In Europe/Australia there is an alternative proposal for a 10m class spectroscopic instrument (WST) (Pasquini et al. 2018)

Schelgel et al. arXiv:2209.04322, arXiv:2209.03585, arXiv:1907.11171

Summary

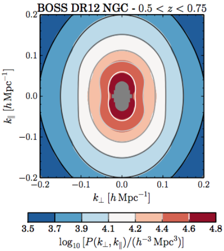

1. Galaxy surveys offer many observational signatures which can be used to constrain cosmological models (some are more robust than others)

Summary

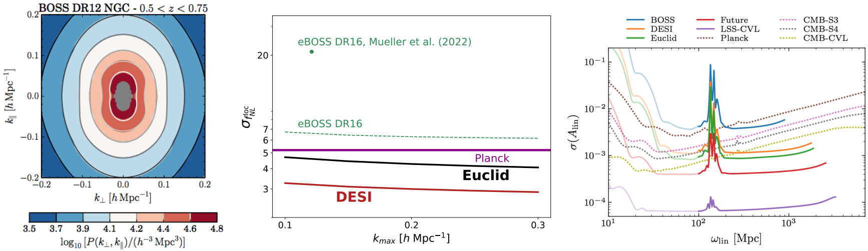

1. Galaxy surveys offer many observational signatures which can be used to constrain cosmological models (some are more robust than others)
2. Stage 4 galaxy redshift surveys (like the **ongoing** DESI and Euclid) have the potential to compete with the CMB on several tests of inflation
3. Galaxy survey constraints on the Hubble constant agree well with the CMB (relying on the same physics but different systematics)

Theoretical systematics of BAO

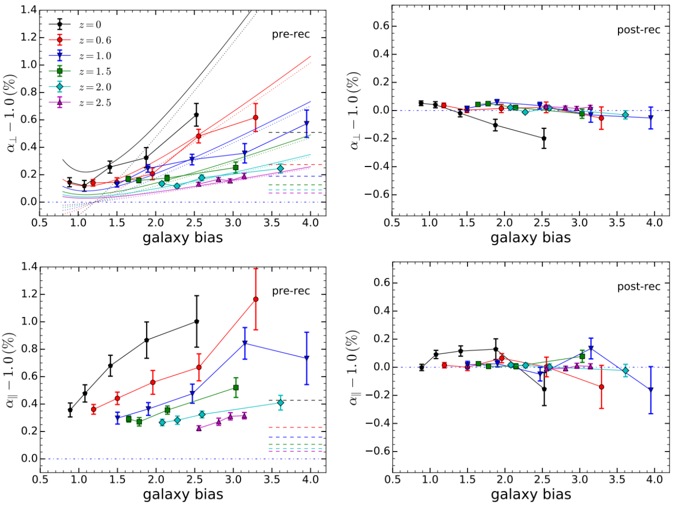

Theoretical systematics of BAO

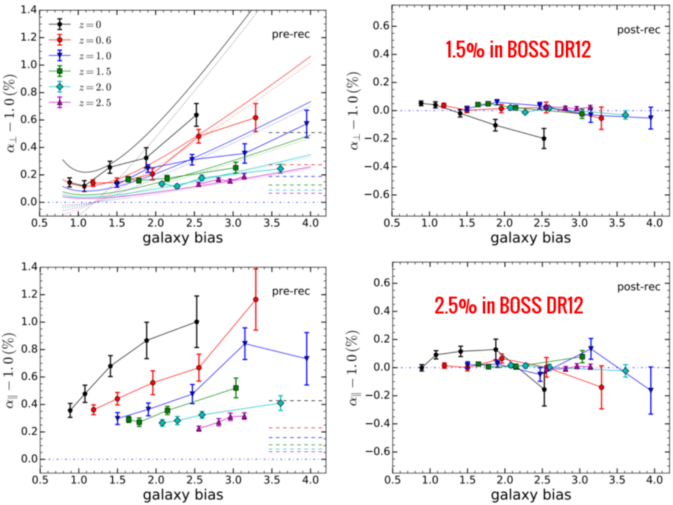

Neutrinos in the CMB Spectrum

Current constraints are dominated by the damping of the power spectrum (degenerate with helium fraction).

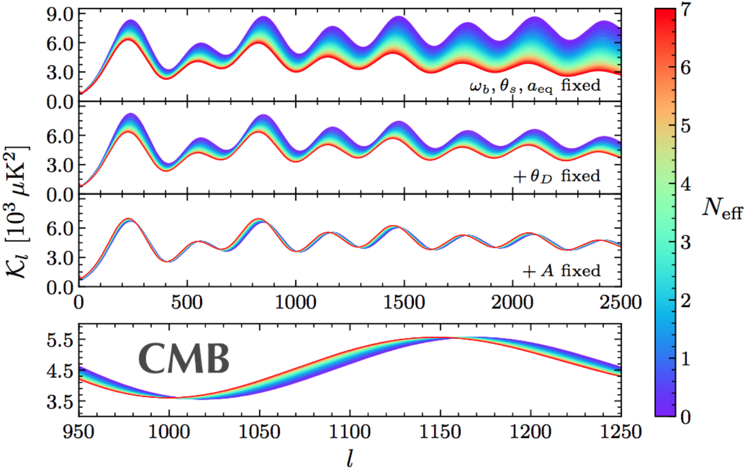

Baumann et al. (2017)

Neutrinos in the BAO Spectrum

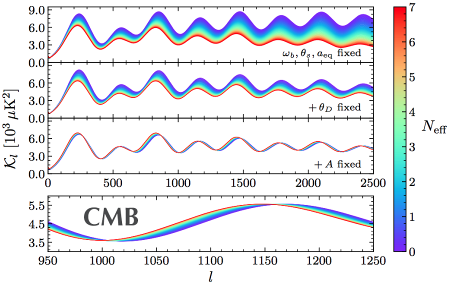

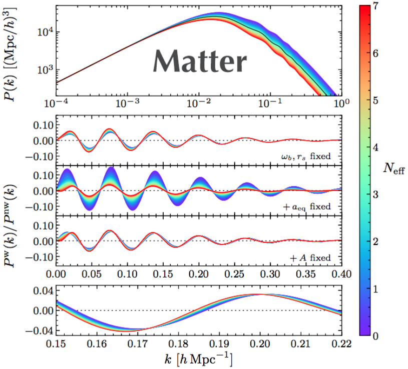

Baumann et al. (2017)

Neutrinos in the BAO Spectrum

$$O(k) = O_{\rm lin}(k/\alpha + (\beta - 1)f(k)/r_s^{\rm fid})e^{-k^2\sigma_{\rm nl}^2/2}$$

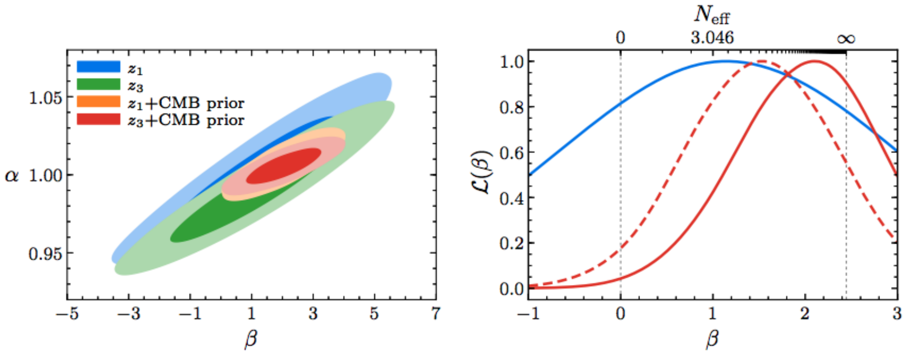

$$\beta(N_{\rm eff}) = \frac{\epsilon}{\epsilon_{\rm fid}} \quad \text{with} \quad \epsilon = \frac{N_{\rm eff}}{8(11/4)^{4/3}/7 + N_{\rm eff}}$$

→ This is a proof of principle for extracting information on light relics from galaxy clustering data.

Baumann + FB++ (2019)

Neutrinos in the BAO Spectrum

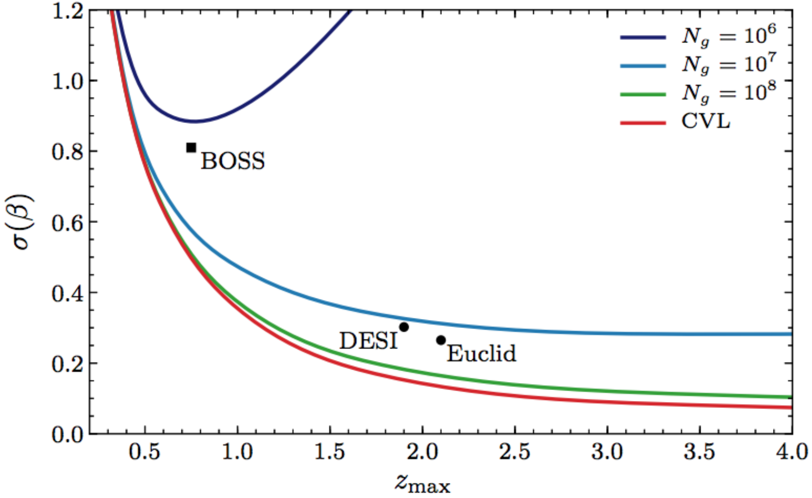

Baumann, FB++ (2019)

First measurement of the anisotropic bispectrum in BOSS

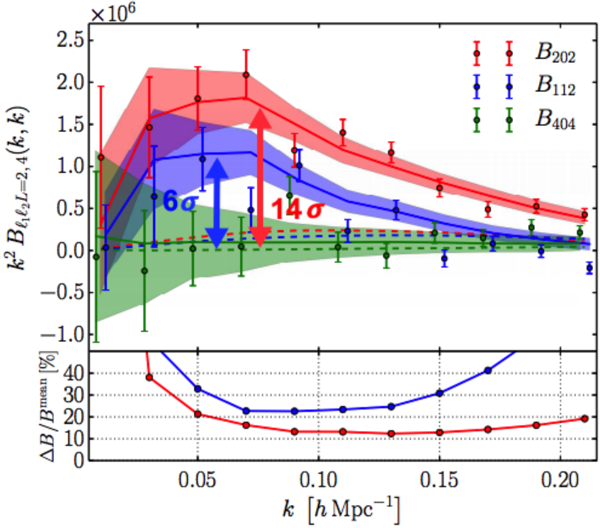

Sugiyama, FB++ (2019)

Bispectrum and RSD forecast (preliminary)

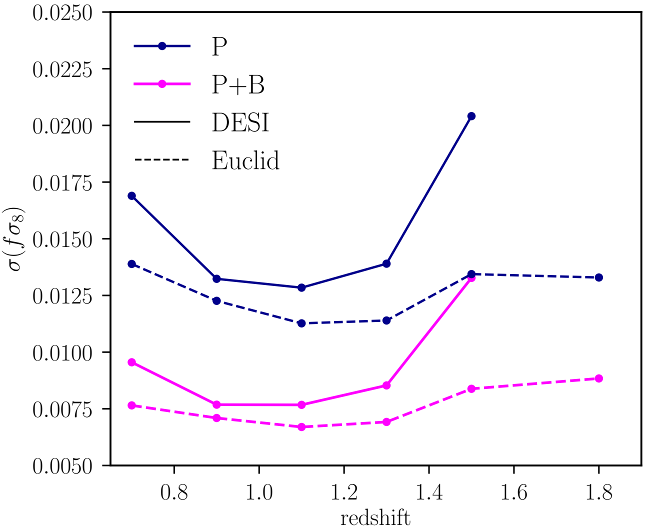

Sugiyama, FB++ (in prep.)

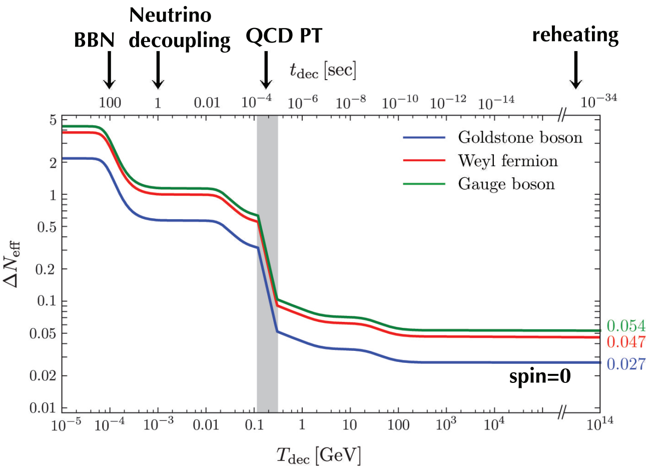

$$\rho_r = \left[1 + \frac{7}{8}\left(\frac{4}{11}\right)^{4/3} N_{\rm eff}\right]\rho_\gamma$$

Baumann et al. (2017)

Motivation: Neutrinos in the phase of the BAO

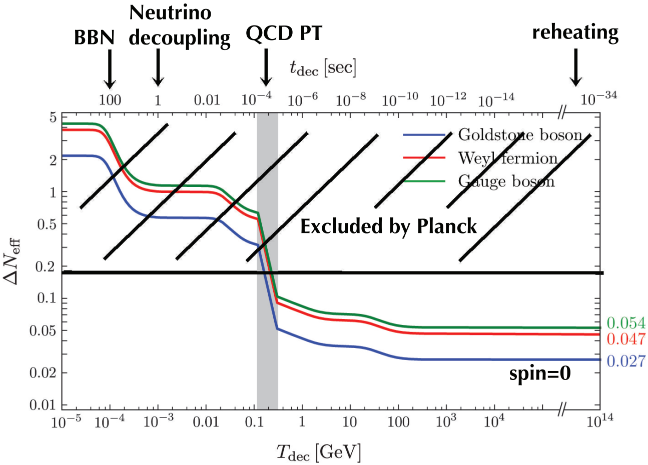

$$N_{\rm eff} = 3.04 \pm 0.18 \qquad \text{(Planck)}$$

Baumann et al. (2017)

Motivation: Neutrinos in the phase of the BAO

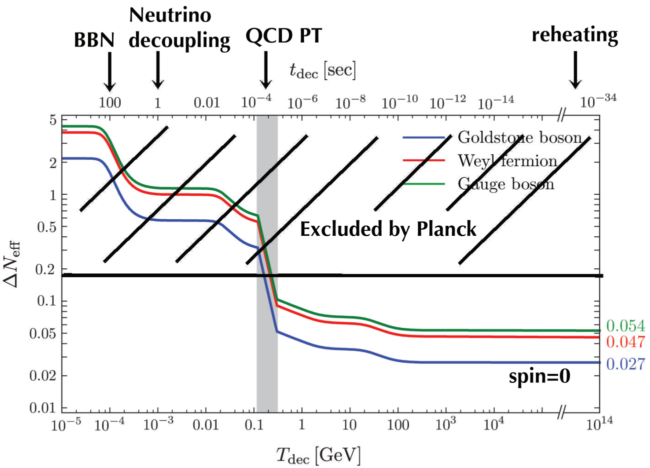

$\sigma(N_{eff}) = 0.030$ (CMB-S4)

$\sigma(N_{eff}) = 0.027$ (CMB-S4 + Euclid)

Baumann et al. (2017)

Fitting the BAO

- Start with linear $P(k)$ and separate the broadband shape, $P^{\rm sm}(k)$, and the BAO feature $O^{\rm lin}(k)$. Include a damping of the BAO feature:

$$P^{\rm sm,lin}(k) = P^{\rm sm}(k)\left[1 + (O^{\rm lin}(k/\alpha) - 1)e^{-k^2\Sigma^2_{\rm nl}/2}\right]$$

- Add broadband nuisance terms

$$A(k) = a_1 k + a_2 + \frac{a_3}{k} + \frac{a_4}{k^2} + \frac{a_5}{k^3}$$
$$P^{\rm fit}(k) = B^2 P^{\rm sm,lin}(k/\alpha) + A(k)$$

- Marginalize to get $\mathcal{L}(\alpha)$.

Relic neutrinos make up 41% of the radiation density

$$\rho_r = \left[1 + \frac{7}{8}\left(\frac{4}{11}\right)^{4/3} N_{\text{eff}}\right] \rho_\gamma$$

CMB

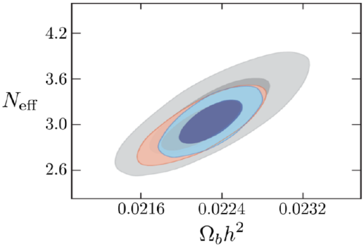

$N_{\text{eff}}^{\text{CMB}} = 3.04 \pm 0.18$

BBN

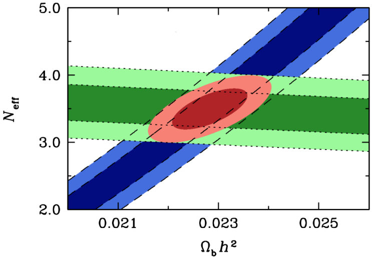

$N_{\text{eff}}^{\text{BBN}} = 3.28 \pm 0.28$

Planck (2015), Cooke et al. (2015)

New decomposition formalism for the bispectrum

The estimator is based on the spherical harmonics expansion

$$
\begin{aligned}
\widehat{B}_{\ell_1\ell_2 L}(k_1,k_2) = H_{\ell_1\ell_2 L} \sum_{m_1 m_2 M} & \begin{pmatrix} \ell_1 & \ell_2 & L \\ m_1 & m_2 & M \end{pmatrix} \\
& \times \frac{N_{\ell_1\ell_2 L}}{I} \int \frac{d^2\hat{k}_1}{4\pi} y_{\ell_1}^{m_1*}(\hat{k}_1) \int \frac{d^2\hat{k}_2}{4\pi} y_{\ell_2}^{m_2*}(\hat{k}_2) \\
& \times \int \frac{d^3k_3}{(2\pi)^3}(2\pi)^3\delta_{\mathrm{D}}\left(\vec{k}_1+\vec{k}_2+\vec{k}_3\right) \\
& \times \delta n(\vec{k}_1)\,\delta n(\vec{k}_2)\,\delta n_L^M(\vec{k}_3)
\end{aligned}
$$

where y_L^{M*}-weighted density fluctuation

$$
\begin{aligned}
\delta n_L^M(\vec{x}) &\equiv y_L^{M*}(\hat{x})\,\delta n(\vec{x}) \\
\delta n_L^M(\vec{k}) &= \int d^3x \mathrm{e}^{-\mathrm{i}\vec{k}\cdot\vec{x}}\delta n_L^M(\vec{x})
\end{aligned}
$$

and $y_\ell^m = \sqrt{4\pi/(2\ell+1)}\,Y_\ell^m$.

Why using this formalism

- This decomposition compresses the data into 2D quantities $B_{\ell_1\ell_2 L}(k_1, k_2)$ rather than 3D quantities like other decompositions $B^m_\ell(k_1, k_2, k_3)$. This reduces the size of the connected covariance matrix.
- This decomposition allows for a self consistent inclusion of the survey window function.
- The RSD information is clearly separated into the L multipoles.
- The complexity of our estimator is $\mathcal{O}((2\ell_1 + 1)N_b^2 N \log N)$.
- Only some multipoles are non-zero: (1) $\ell_1 > \ell_2$ (2) L = even (3) $|\ell_1 - \ell_2| \leq L \leq |\ell_1 + \ell_2|$ and (4) $\ell_1 + \ell_2 + L =$ even.